

Colloid Formation by Drugs in Simulated Intestinal Fluid

Allison K. Doak,[†] Holger Wille,^{‡,§} Stanley B. Prusiner,^{‡,§} and Brian K. Shoichet^{*†}

[†]Department of Pharmaceutical Chemistry, University of California—San Francisco, 1700 4th Street, San Francisco, California 94158-2550,

[‡]Institute for Neurodegenerative Diseases, and [§]Department of Neurology, University of California—San Francisco, San Francisco, California 94143-0518

Received February 25, 2010

Many organic molecules form colloidal aggregates in aqueous solution at micromolar concentrations. These aggregates promiscuously inhibit soluble proteins and are a major source of false positives in high-throughput screening. Several drugs also form colloidal aggregates, and there has been speculation that this may affect the absorption and distribution of at least one drug in vivo. Here we investigate the ability of drugs to form aggregates in simulated intestinal fluid. Thirty-three Biopharmaceutics Classification System (BCS) class II and class IV drugs, spanning multiple pharmacological activities, were tested for promiscuous aggregation in biochemical buffers. The 22 that behaved as aggregators were then tested for colloid formation in simulated intestinal fluid, a buffer mimicking conditions in the small intestine. Six formed colloids at concentrations equal to or lower than the concentrations reached in the gut, suggesting that aggregation may have an effect on the absorption and distribution of these drugs, and potentially others, in vivo.

Early drug discovery suffers from a high rate of false positives. This problem is particularly acute in high-throughput screening.^{1–5} Many of these false positive “hits” are attributed to promiscuously inhibiting colloidal aggregates, which are spontaneously formed by many organic molecules in aqueous solution.^{6–9} Once formed, these aggregates nonspecifically inhibit protein by sequestration and partial denaturation.^{2,10} Originally considered a problem of screening, it became apparent that most classes of bioactive organic small molecules could form colloidal aggregates at micromolar concentrations. In succession, it was shown that probe molecules such as kinase inhibitors,^{11–13} natural products such as quercetin² and adociasulfate-2,⁹ and even drugs such as nicardipine, delavirdine, clotrimazole, and cinnarizine^{14,15} could form colloids. As disconcerting as it was to find aggregating drugs, this was thought to be a problem relevant only for screening conditions in biochemical buffers and not for in vivo effects.

Subsequently, however, Arnold, Janssen, and colleagues argued that aggregation may indeed affect the distribution of oral drugs in vivo.^{16–18} After observation that some hydrophobic non-nucleoside reverse transcriptase inhibitors (NNRTIs^a) showed surprisingly high bioavailability in vivo, their pharmacokinetic and physicochemical properties were investigated.^{16–18} Many compounds from the diarylthiazine/diarylpyrimidine classes of NNRTIs were shown to aggregate in gastric-mimicking conditions, with a distinct particle size difference between highly and poorly absorbed compounds (radii from 30 to 100 nm and > 250 nm, respectively).^{16,18} A model of aggregate absorption into the lymphatic pathway via microvilli (M) cells in Peyer’s patches in the small intestine

was proposed. To test this hypothesis in vivo, the diarylpyrimidine dapivirine was administered orally to dogs, and drug concentrations in the lymph fluid and plasma were compared; at 2 h, the lymph concentration was 3 times that of plasma, consistent with primary absorption via the lymphatic system, perhaps as colloidal aggregates.¹⁸ In response to these findings, experiments were conducted to show that colloidal aggregates are unperturbed by high concentrations of protein as found in biological environments, supporting the idea that stable colloid formation may be possible in vivo.¹⁹

Two questions emerge from these observations. First, how many drugs aggregate in conditions encountered in the GI tract? Second, how would such aggregation affect their absorption and distribution? The second question is challenging to address, but as a preliminary step, it seemed useful to investigate the ability of a broad range of oral drugs, mostly BCS class II and class IV low solubility drugs, to aggregate in a buffer simulating the conditions of the small intestine. Thirty-three marketed oral drugs, covering many biological activities, were first tested for aggregation in biochemical buffers by measuring particle formation and aggregation-based inhibition. Those that formed colloids were then tested for aggregation in fed state simulated intestinal fluid (FeSSIF). Drugs were assayed for particle formation up to concentrations that would be found in the gut following oral administration. To test whether the particles detected by light scattering share the same properties as previously characterized colloidal aggregates,^{2,14,15} sedimentation assays were conducted and aggregates were visualized by transmission electron microscopy. We consider the implications of these observations and the further studies on actual in vivo distribution that they suggest.

Results

Thirty-three diverse oral drugs were tested for colloid formation in biochemical buffers (Figure 1). We chose low

*To whom correspondence should be addressed. Phone: 415-514-4126. Fax: 415-514-4260. E-mail: shoichet@cgl.ucsf.edu.

^aAbbreviations: BCS, Biopharmaceutics Classification System; CAC, critical aggregation concentration; DLS, dynamic light scattering; FeSSIF, fed state simulated intestinal fluid; NNRTI, non-nucleoside reverse transcriptase inhibitor.

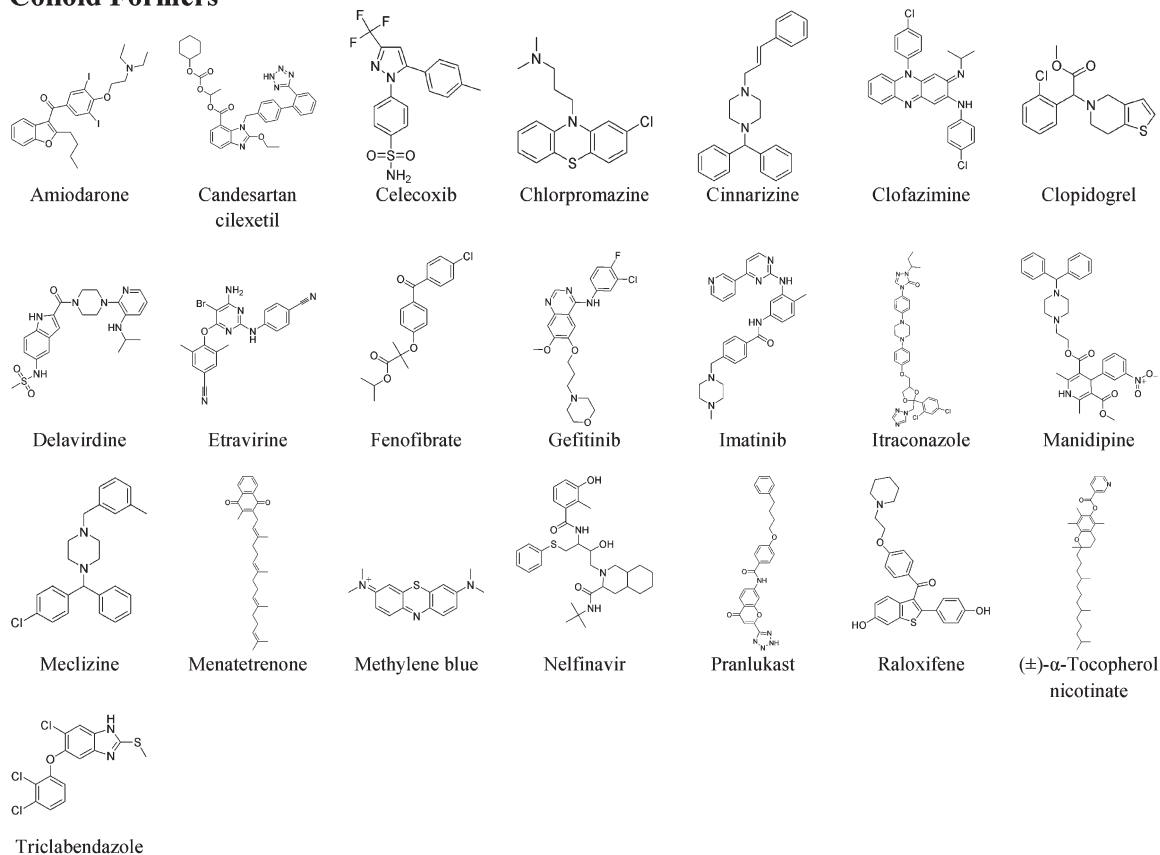
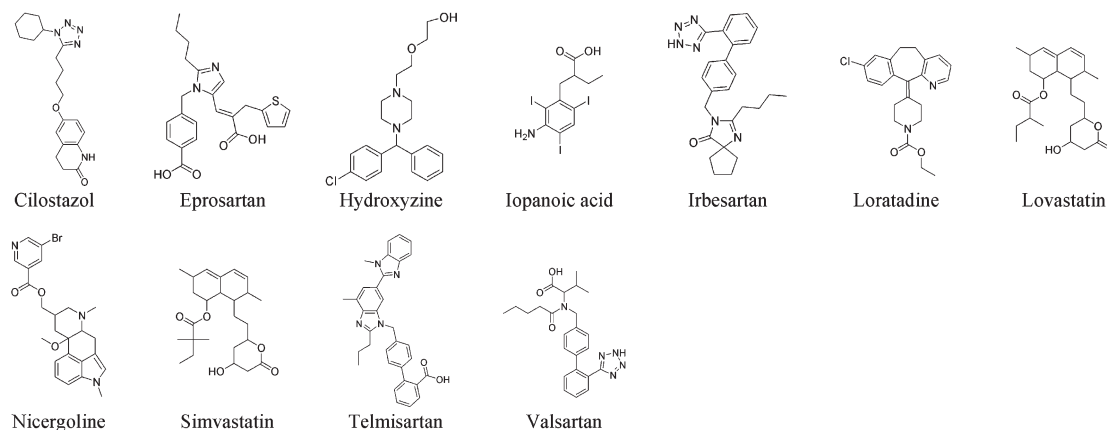
Colloid Formers**Non-Colloid Formers**

Figure 1. Chemical structures of drugs tested for aggregation in biochemical buffers.

solubility drugs with high ClogP values, as they are more prone to aggregation than high solubility drugs.¹⁵ We also tested methylene blue, a dye used in several clinical indications and now in clinical trials for treatment of Alzheimer's disease.^{20–22} Two criteria were used to characterize colloid-forming drugs: particle formation and detergent-reversible enzyme inhibition.^{7,23–25} Drugs were tested up to concentrations that would be found in the small intestine after oral administration. These concentrations were calculated using maximum dosage information and assuming a small intestine volume of 1 L.^{26–28} We note that this volume is among the higher estimates, with recent studies reporting volumes closer to 300 mL or even lower.^{29–32} Thus, we believe these concentrations to be conservative to the low side. Particle radii were measured by dynamic light scattering

(DLS), and IC₅₀ values were measured against cruzain in the presence and absence of Triton X-100. The cruzain inhibition assay was used instead of the classical aggregation-based AmpC β -lactamase inhibition assay because the fluorogenic reporting system allows for a more efficient high-throughput setup. Several compounds were limited by solubility in the cruzain assay; in these cases, inhibition never reached 50%, and the IC₅₀ values were reported as greater than the highest soluble concentration tested. Of the 33 drugs assayed, 22 drugs formed colloids in biochemical buffers (Table 1, Figure 1). Drugs classified as noncolloid formers did not meet one or both criteria for colloid formation.

To investigate whether colloid-forming drugs can also form aggregates under in vivo-like conditions, we tested the 22 drugs

Table 1. Colloid Formation in Biochemical Buffers

drug	IC ₅₀ vs cruzain ^a (μM)		DLS concn ^b (μM)	colloid radius ± SD (nm)
	no Triton X-100	0.01% Triton X-100		
amiodarone	4	206 ^c	2	64.0 ± 12.0
candesartan	42	168 ^c	50 ^d	38.8 ± 10.1
cilexetil				
celecoxib	126	> 400	120 ^e	161.8 ± 14.0
chlorpromazine	189	284	500	29.2 ± 0.8
cinnarizine ^f	124	> 300 ^c	10	89.1 ± 10.6
clofazimine	6	40	10	356.1 ± 18.9
clopidogrel	123	> 300	60 ^g	48.3 ± 2.0
sulfate				
delavirdine ^f	122	> 200	100 ^h	195.1 ± 22.5
etravirine ^f	4	> 200	10	323.2 ± 14.1
fenofibrate	61	> 500	10	129.0 ± 6.8
gefitinib	88	148	250 ^h	160.1 ± 11.4
imatinib	207	297	100	118.4 ± 19.2
itraconazole	3	> 200	2.5	138.1 ± 8.3
manidipine	6	> 100	2.5	125.6 ± 7.3
meclizine	129	> 250	5	133.3 ± 7.5
menatetrenone	18	> 200	5	72.5 ± 6.1
methylene blue	55	85	20	95.9 ± 12.5
nelfinavir	144	> 300	20	690.7 ± 217.2
pranlukast	7	68 ^c	50	1167.7 ± 293.8
raloxifene	33	128 ^c	20	192.2 ± 20.2
(±)-α-tocopherol	98	> 400	10	104.1 ± 3.3
nicotinate				
tricalabendazole	15	> 200	10	93.0 ± 5.1

^a 95% confidence intervals are listed in Supporting Information Table 1. ^b Indicates the drug concentration at which DLS measurements were made. 1% DMSO was used unless otherwise noted. ^c 0.1% Triton X-100. ^d 0.25% DMSO. ^e 0.6% DMSO. ^f Previously published aggregator. ^g 0.3% DMSO. ^h 0.5% DMSO.

in fed state simulated intestinal fluid (FeSSIF), a buffer widely used for drug dissolution studies.^{27,33–35} FeSSIF is designed to mimic the conditions in the small intestine following meal ingestion. This biorelevant medium differs from the buffer used by Frenkel et al. to investigate aggregate formation by NNRTIs. Whereas their group simulated gastric conditions,¹⁶ we simulated intestinal conditions to more closely resemble the environment of potential aggregate absorption via Peyer's patches located in the small intestine.^{27,28} Particle formation in FeSSIF was measured by DLS. Six drugs (18% of total drugs included in this study, 27% of colloid formers in biochemical buffers) formed particles in FeSSIF at concentrations substantially lower than would be present in the gut following oral administration (Table 2). Because of the high content of taurocholate, FeSSIF contained micelles that add to the light scattering measured by DLS. To verify that colloidal particles were distinguishable from this background, standard calibration beads ($r = 200$ nm) were diluted in FeSSIF and light scattering was measured. As seen in Figure 2C, the bead-containing samples exhibited strong autocorrelation curves of a clearly different shape than FeSSIF without beads. The six drugs that aggregated in FeSSIF showed strong curves similar to the bead-containing samples and distinct from FeSSIF background, consistent with the presence of colloidal aggregates (Figure 2B).

To ensure that the large particles observed by DLS were indeed colloidal aggregates, their properties were compared to previously characterized aggregates. A distinguishing characteristic of colloidal aggregates is their critical aggregation concentration (CAC) at which colloids will form; compound

below that CAC will remain in true solution in monomeric form. Upon centrifugation, the colloids will be pelleted out of solution while the monomeric molecules will remain in the supernatant.^{2,14} Samples of itraconazole (35 μM, 0.35% DMSO) and delavirdine (750 μM, 3% DMSO) in FeSSIF were centrifuged; their CAC values are 6.9 ± 1.9 and 488.3 ± 31.0 μM, respectively. Consistent with the formation of colloidal aggregates, these drugs were pelleted out of solution in FeSSIF in a CAC-dependent manner as demonstrated by the percent of each drug collected in the pellet (Figure 3).

Additionally, colloid formers have been shown to interact directly with protein in biochemical buffers.^{2,10} To investigate whether or not this interaction also occurs in FeSSIF, we analyzed β-lactamase cosedimentation with colloid forming drugs. Itraconazole and delavirdine were incubated with 2 μg of β-lactamase in FeSSIF and centrifuged to pellet colloids out of solution. If β-lactamase binds to the colloid surface, the protein will be pelleted with the drug, whereas unbound protein will remain in the supernatant. The large amount of protein in drug-containing pellets (lanes 6 and 9) versus β-lactamase alone (lane 3) indicates that colloids do bind protein in FeSSIF (Figure 4). Pellets of drug samples without protein were included in the SDS-PAGE gel (lanes 4 and 7) to ensure that drug alone did not cause background in the silver staining.

If drugs form colloids in FeSSIF, they should be visible by transmission electron microscopy and distinguishable from precipitate, which would appear microcrystalline in structure. We compared aggregates of itraconazole, delavirdine mesylate, and methylene blue in phosphate buffer to those formed in FeSSIF (Figure 5). Though there are strong backgrounds of phospholipid structures in the FeSSIF samples, the colloidal aggregates are readily visible over this background. By shape and general appearance, the particles in FeSSIF resemble their counterparts in phosphate buffer, as well as previously published micrographs of aggregating compounds,^{2,16–18} and are clearly not in a precipitated form. The colloids formed in FeSSIF are visibly smaller than those formed in phosphate buffer, complementing the results obtained by light scattering.

Discussion

Oral drugs have stringent solubility and permeability constraints,³⁶ and so it may seem baffling that so many form colloidal aggregates in simple buffers or that any do so in simulated intestinal fluid. Nevertheless, those are the central observations of this study. Of the 33 drugs tested, 22 aggregated at relevant concentrations in phosphate buffer (67%) and 6 did so in FeSSIF (18% of total drugs tested; 27% of colloid formers). Admittedly, these oral drugs were chosen for their low solubility BCS classifications; thus, we were examining a biased set. Also, the earlier work by Arnold, Janssen, and colleagues on the diarylpyrimidine NNRTIs^{16–18} and our own studies on drug aggregation¹⁵ suggested that it was at least plausible that some drugs would behave this way. That so many did so, across pharmacological classes, surprised us. Since aggregation is concentration and condition dependent, this behavior and its implications merit close scrutiny.

Many of the drugs studied here, like imatinib, celecoxib, amiodarone, and meclizine, are household names and have been taken by hundreds of millions of people. In phosphate buffer there is little doubt that they form colloidal aggregates. They scatter light intensely by DLS, with well-formed autocorrelation curves consistent with particle sizes in the 100–500 nm

Table 2. Colloid Formation in Simulated Intestinal Fluid^a

Drug	Conc. in small intestine ^b (μM)	DLS conc. (μM)	Radius (nm)
Delavirdine	724	600 ^c	62.8 \pm 33.0
Etravirine	460	200	373.3 \pm 150.6
Itraconazole	142	20	64.5 \pm 4.8
Menatetrenone (Vitamin K ₂)	100	20 ^d	36.8 \pm 5.7
Methylene blue	347	150 ^e	52.6 \pm 20.8
Tocopherol	373	50	55.7 \pm 2.9

^aDLS measurements were made using 1% DMSO unless otherwise noted. ^bCalculated using maximum drug dosage and 1 L volume in small intestine. ^c3% DMSO. ^d0.2% DMSO. ^e0.75% DMSO.

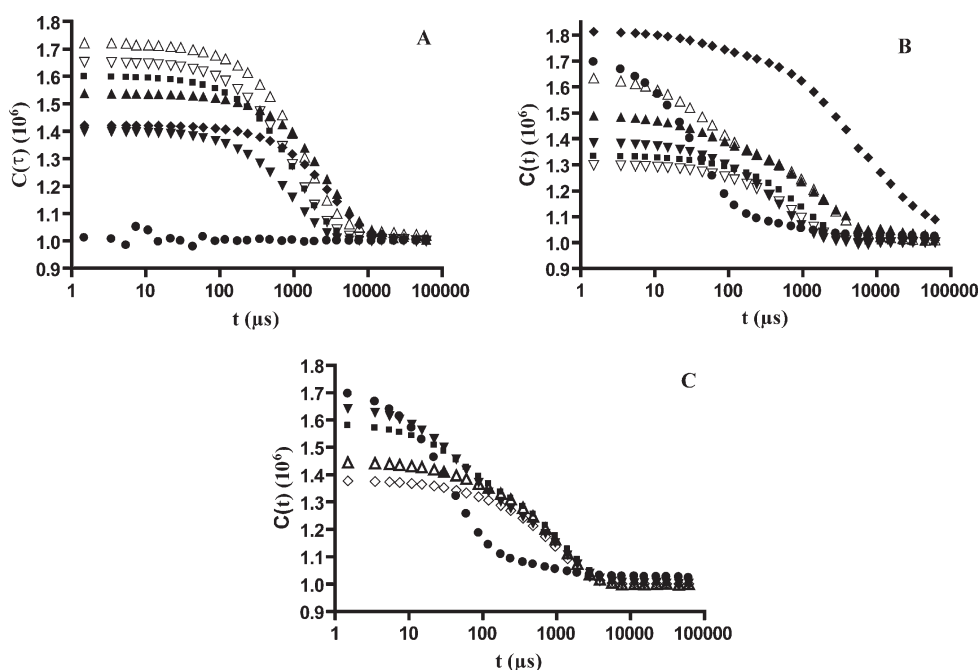


Figure 2. Autocorrelation curves from DLS showing (A) drugs in 50 mM phosphate buffer and (B) in FeSSIF: (●) KPi, (▼) tocopherol nicotinate, (◆) etravirine, (▲) delavirdine, (■) menatetrenone, (▽) itraconazole, (△) methylene blue. (C) Calibration beads in FeSSIF: (●) FeSSIF, (▼) 15 fM beads, (◆) 60 fM beads, (▲) 240 fM beads, (■) 480 fM beads. Each curve is one representative sample from each set.

size range (Figure 2A), as has been observed previously for other classes of molecules. They inhibit the reporter enzyme cruzain²⁴ at low to mid-micromolar concentrations, and this inhibition can be reversed with low concentrations of the non-ionic detergent Triton X-100 (Table 1). This has two implications. First, panels of drugs are often first choices when screening

against a new target because they are expected to have good physicochemical properties and because they are information-rich molecules. Whereas this logic remains sound, a lesson from this study is that they offer no panacea; drugs and other biomolecules²⁴ can form colloidal aggregates under screening-relevant conditions, and when they do so, they are prone to

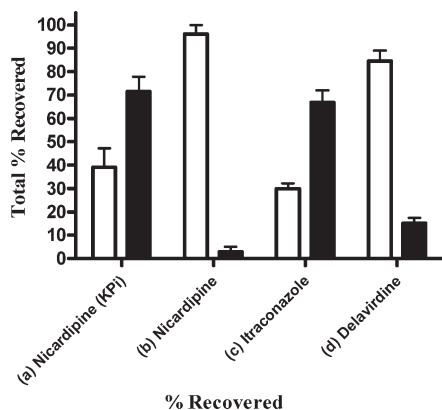


Figure 3. UV-visible quantification of colloids pelleted from FeSSIF by centrifugation. Bars illustrate the percent found in the (□) supernatant and (■) pellet: (a) nicardipine (60 μ M), a previously described strong aggregator, in 50 mM KPi; (b) nicardipine (60 μ M), which is not observed to form colloids in FeSSIF; (c) itraconazole (35 μ M); (d) delavirdine mesylate (750 μ M).

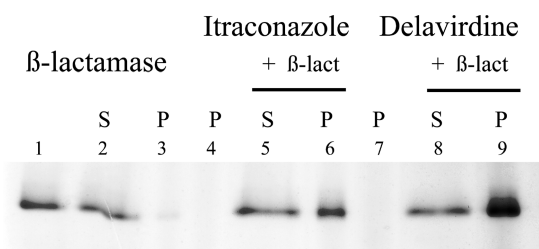


Figure 4. β -Lactamase cosediments with colloids in FeSSIF. Lane 1 is 2 μ g of β -lactamase in 1 mL of FeSSIF, without centrifugation. Lanes 2 and 3 are the supernatant (S) and pellet (P), respectively, from centrifugation of β -lactamase alone. Lanes 4 and 7 are the pellets from centrifugation of each colloid-forming drug alone. Lanes 5 and 8 are the supernatants, and lanes 6 and 9 are the pellets of β -lactamase incubated with colloid forming drugs.

induce screening artifacts. Second, aggregation in the intestine may be more common even than what we describe here. We have used conservative estimates for the maximum concentration reached by drugs in the intestine, assuming a 1 L volume for this compartment. Had we chosen lower volumes, as recently reported,^{29–32} the maximum concentration would have been higher and so their likelihood of aggregating. For instance, drugs like candesartan, clofazimine, and fenofibrate, which do not aggregate in FeSSIF at the lower concentrations used here, begin to do so at higher concentrations (Supporting Information Table 2, Supporting Information Figure 1).

Colloid formation in simulated intestinal fluid is harder to assay, largely because of the presence of the detergent-like taurocholate, and since this is the most interesting conclusion of this study we will reprise the observations that support it. Whereas the FeSSIF adds to background light scattering, the DLS curves for the six aggregating drugs in that medium remain clear: the autocorrelation curves are well formed and distinctive from FeSSIF background (Figure 2B). Intriguingly, the radii of the particles are diminished in FeSSIF versus phosphate, consistent with the FeSSIF affecting their character and moving them into a size range where they might be better absorbed by particle-detecting cells of the Peyer's patch, as first suggested by Arnold, Janssen, and colleagues.¹⁶ As with well-studied, "classical" colloid formers, such as tetraiodophenolphthalein and nicardipine, drugs like itraconazole and delavirdine may be pelleted out of FeSSIF by centrifugation

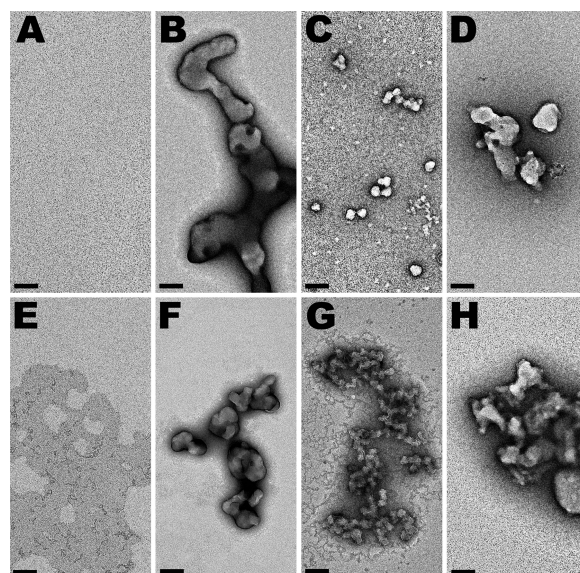


Figure 5. Negative stain electron microscopy of colloid-forming compounds. (A) Phosphate buffer is shown with homogeneous background without particulates. (B) Itraconazole in phosphate buffer forms large colloids, while under the same conditions methylene blue (C) and delavirdine mesylate (D) form small and intermediate sized colloids, respectively. (E) Negatively stained FeSSIF reveals only low-contrast lipid and detergent structures based on the taurocholate and lecithin content. Itraconazole (F), methylene blue (G), and delavirdine mesylate (H) retain their colloid forming ability in FeSSIF, forming colloids similar to those seen in phosphate buffer. The contrast for panels B, C, D, G, and H was adjusted nonlinearly by using a high-pass Fourier filter to reduce the intensity of the negative stain. Bar = 100 nm.

when they reach concentrations above their CAC, whereas they cannot be pelleted out when below their CAC values. Additionally, these pelleted colloids can pull protein down with them, which indicates a direct colloid–protein interaction, as previously demonstrated.² Finally, drugs like itraconazole, delavirdine, and methylene blue form distinct spheroidal particles, in the 100 nm size range, by negative staining transmission electron microscopy. Although these particles must be disentangled from a background of lipid/detergent structures in FeSSIF, this may be done without strain, as the lecithin and taurocholate form thin layers of lipid/detergent structures while the drug colloids stand out by their dimensionality, shape, and size. Taken together, these observations leave little room for doubt that 6 of the 33 drugs studied here, delavirdine, etravirine, itraconazole, menatetrenone, methylene blue, and tocopherol, form colloidal aggregates in a medium widely accepted to mimic the fed state of the small intestine.

Certain caveats, codicils, and conditions merit airing. We have shown that six drugs form colloids in FeSSIF at concentrations likely to be reached at or below their highest administered dose, taking a conservative (high) estimate of fed-state small intestine volume, and another three drugs do so at higher concentrations. Still, it remains true that many do not form colloids in FeSSIF, even from the biased group of oral drugs from which the 33 were drawn. We do not argue that this effect applies to most drugs or even, at least at this stage, very many. Our results do not, at this point, suggest even a physical SAR around which drugs might aggregate in FeSSIF. Whereas low solubility BCS class II and class IV oral drugs, from which most of those tested here were drawn, seem more likely to aggregate under these conditions, those that did

so in FeSSIF span a wide range of ClogP values and molecular weights, with both the most lipophilic (menatetrenone and tocopherol) and the most hydrophilic (delavirdine and methylene blue) and several in the midrange forming colloids, while physically related compounds do not. Nor do we pretend, even for the six drugs that do aggregate in FeSSIF, that this means they do so in the intestine; far less have we shown that they are absorbed as colloidal particles into systemic, lymphatic circulation. Doing so will demand more detailed, physiologically relevant studies in animals. What this study does sustain is the reasonability of this hypothesis, first aired by others,^{16,18} for some oral drugs. Certainly the observation that these six drugs form colloidal aggregates in simulated intestinal fluid is strongly supported by multiple lines of evidence. If drugs do form colloids in the small intestine, it could affect their absorption and distribution, either by delaying these processes or by changing distribution sites and time courses. It goes without saying that these are critical aspects of drug pharmacokinetics and efficacy. A key result of this study is that the drug aggregation in the small intestine remains a reasonable hypothesis, and its effects on drug behavior would be so fundamental as to merit further study in physiologically relevant systems.

Materials and Methods

Materials. Cruzain was expressed and purified as previously described.³⁷ Duke Standards NIST traceable polymer microspheres, 200 nm in diameter, were purchased from Thermo Scientific. Amiodarone hydrochloride, cinnarizine, clofazimine, fenofibrate, menatetrenone, methylene blue, nicardipine hydrochloride, (\pm)- α -tocopherol nicotinate, trichloroethylene, chlorpromazine hydrochloride, hydroxyzine dihydrochloride, nicotholone, taurocholic acid sodium salt hydrate, and L- α -lecithin (from egg yolk) were purchased from Sigma-Aldrich. Celecoxib, clopidogrel sulfate, imatinib, itraconazole, manidipine, candesartan cilexetil, eprosartan mesylate, irbesartan, loratadine, lovastatin, telmisartan, and valsartan were purchased from AK Scientific. Pramlanast, raloxifene hydrochloride, and simvastatin were purchased from US Biological. Delavirdine mesylate was purchased from BIOMOL International, meclizine dihydrochloride from MP Miomedicals, cilostazol from Bosche Scientific, LLC, gefitinib from LC Laboratories, iopanoic acid from TCI American, and nelfinavir from Ryan Scientific. Most of the drugs chosen for this study were BCS class II and class IV drugs with ClogP values greater than 3.5.

FeSSIF Preparation. Blank FeSSIF was prepared by adding 8.65 g of acetic acid and 15.2 g of potassium chloride to deionized water. Sodium hydroxide was added until pH 5.0 was reached. Full media were prepared fresh each day. Blank FeSSIF was filtered through a 0.22 μ m filter, and sodium taurocholate and lecithin were added to 15 and 3.75 mM, respectively, and dissolved by heating to 37 °C and vortexing.

Dynamic Light Scattering. Concentrated DMSO stocks of drugs were diluted with filtered 50 mM KPi, pH 7.0, or FeSSIF. The final DMSO concentration was 1% unless otherwise noted. Measurements were made using a DynaPro MS/X (Wyatt Technology) with a 55 mW laser at 826.6 nm. The laser power was 100%, and the detector angle was 90°. Each diameter value reported represents the average of three or more independent measurements at room temperature. The compositions of samples in phosphate buffer in Figure 2 are 10 μ M tocopherol nicotinate, 1% DMSO; 10 μ M etravirine, 1% DMSO, 100 μ M delavirdine, 0.5% DMSO, 1 μ M menatetrenone, 0.01% DMSO, 1 μ M itraconazole, 0.04% DMSO, and 30 μ M methylene blue, 0.06% DMSO; and in FeSSIF are 100 μ M tocopherol nicotinate, 0.4% DMSO, 150 μ M etravirine, 0.6% DMSO, 600 μ M delavirdine, 3% DMSO, 5 μ M menatetrenone, 1% DMSO, 20 μ M

itraconazole, 0.2% DMSO, and 200 μ M methylene blue, 2% DMSO. Figure 5 shows results from 600 μ M clofazimine, 6% DMSO; 550 μ M candesartan cilexetil, 2.75% DMSO; and 450 μ M fenofibrate, 1.8% DMSO.

Cruzain Assay. Cruzain assays were performed in 100 mM sodium acetate, pH 5.5, containing 5 mM DTT. Triton X-100 was added to 0.01% or 0.1% in reaction mixtures as needed. Drugs were incubated with 0.8 nM cruzain for 5 min until reactions were initiated by adding the fluorogenic substrate Z-Phe-Arg-aminomethylcoumarin (Z-FR-AMC). The final reaction volume was 200 μ L with cruzain at 0.4 nM and Z-FR-AMC at 2.5 μ M. Final DMSO concentrations were generally 0.5% and no greater than 5%, depending on the range of the drug concentration investigated. To measure enzyme inhibition, the increase in fluorescence (excitation wavelength of 355 nm, emission wavelength of 460 nm) was recorded for 5 min in a microtiter plate spectrofluorimeter (Molecular Devices, FlexStation). Assays were performed in duplicate in 96-well plates, with controls measuring enzyme activity in the presence of DMSO. Activity was measured for at least seven different concentrations for each drug. Dose–response curves were plotted, and IC₅₀ values and corresponding 95% confidence intervals were calculated using GraphPad Prism 4 (GraphPad, San Diego, CA), using a sigmoidal dose–response curve analysis with variable slope and the bottom constrained to be greater than zero.

Sedimentation Assay. Solutions of nicardipine (60 μ M, 1% DMSO), itraconazole (35 μ M, 0.35% DMSO), and delavirdine mesylate (750 μ M, 3% DMSO) were prepared by diluting concentrated DMSO stocks into 50 mM KPi, pH 7.0, or FeSSIF, with a final volume of 1 mL. Samples were centrifuged at 16000g for 1 h at room temperature. Delavirdine mesylate was centrifuged at 76000g for 1 h. Supernatants were removed and pellets (bottom 10 μ L) were resuspended to 1 mL with DMSO or methanol. UV–visible spectrophotometry was used to determine the concentration of compound in the supernatant and the resuspended pellet. Absorbance was measured at 352 nm for the nicardipine supernatant in phosphate buffer ($\epsilon = 4.6 \times 10^3 \text{ M}^{-1} \text{ cm}^{-1}$), 355 nm for the FeSSIF supernatant ($\epsilon = 6.7 \times 10^3 \text{ M}^{-1} \text{ cm}^{-1}$), and 355 nm for both pellets in DMSO ($\epsilon = 6.4 \times 10^3 \text{ M}^{-1} \text{ cm}^{-1}$). Absorbance was measured at 264 nm for the itraconazole supernatant ($\epsilon = 21.9 \times 10^3 \text{ M}^{-1} \text{ cm}^{-1}$) and at 267 nm for the pellet in DMSO ($\epsilon = 25.9 \times 10^3 \text{ M}^{-1} \text{ cm}^{-1}$). Absorbance was measured at 301 nm for the delavirdine supernatant ($\epsilon = 19.4 \times 10^3 \text{ M}^{-1} \text{ cm}^{-1}$) and pellet in methanol ($\epsilon = 24.3 \times 10^3 \text{ M}^{-1} \text{ cm}^{-1}$). Bars in Figure 3 represent the mean and standard deviation of at least three replicate measurements.

Cosedimentation Assay. Solutions of itraconazole (200 μ M, 2% DMSO) and delavirdine mesylate (700 μ M, 3% DMSO) were prepared as above in FeSSIF, with additional samples also including 2 μ g of AmpC. Samples were centrifuged at 16000g for 30 min at room temperature. After removal of all supernatant liquid, pellets were resuspended with 5 μ L of DMSO plus 5 μ L of 50 mM KPi, pH 7.0, and run on an SDS–PAGE gel. Protein was detected using silver staining.

Negative Staining and Transmission Electron Microscopy. Solutions were prepared by diluting concentrated DMSO stocks of drugs with FeSSIF. The negative staining was performed as previously described.³⁸ In brief, negative staining was done on formvar/carbon coated 200 mesh copper grids (Ted Pella, Inc.; Redding, CA) which were glow discharged prior to staining. Then 5 μ L samples were adsorbed for \sim 30 s and the grids were stained with 2 drops (50 μ L) of freshly filtered 2% ammonium molybdate. After drying, the samples were viewed in a FEI Tecnai F20 electron microscope (Eindhoven, The Netherlands) at 80 kV and a standard magnification of 25000. Electron micrographs were recorded with a Gatan Ultrascan CCD camera. The magnification was calibrated using negatively stained catalase crystals and ferritin. Figure 5 shows 50 μ M itraconazole, 0.5% DMSO, 100 μ M methylene blue, 0.2% DMSO, and 200 μ M delavirdine mesylate, 0.2% DMSO in 50 mM phosphate; and

100 μM itraconazole, 1% DMSO, 200 μM methylene blue, 1% DMSO; and 700 μM delavirdine mesylate, 3% DMSO in FeSSIF.

Acknowledgment. This work was supported by NIH Grant GM71630 and an ARRA Supplement Grant GM71630-5S1 (to B.K.S.) and by Grant AG02132 (S.B.P., PI) and by generous support from the Sherman Fairchild Foundation (to S.B.P.). We thank Rafaela Ferreira, Melody Lee, and Michael Mysinger for reading this manuscript. We also thank Rafaela Ferreira for cruzain purification.

Supporting Information Available: Confidence ranges for inhibition assays, colloid formation of drugs at higher concentrations in FeSSIF are shown, and a figure showing dynamic light scattering in FeSSIF. This material is available free of charge via the Internet at <http://pubs.acs.org>.

References

- (1) Keseru, G. M.; Makara, G. M. Hit discovery and hit-to-lead approaches. *Drug Discovery Today* **2006**, *11*, 741–748.
- (2) McGovern, S. L.; Helfand, B. T.; Feng, B.; Shoichet, B. K. A specific mechanism of nonspecific inhibition. *J. Med. Chem.* **2003**, *46*, 4265–4272.
- (3) Rishton, G. M. Nonleadlikeness and leadlikeness in biochemical screening. *Drug Discovery Today* **2003**, *8*, 86–96.
- (4) Roche, O.; Schneider, P.; Zuegge, J.; Guba, W.; Kansy, M.; Alanine, A.; Bleicher, K.; Danel, F.; Gutknecht, E. M.; Rogers-Evans, M.; Neidhart, W.; Stalder, H.; Dillon, M.; Sjogren, E.; Fotouhi, N.; Gillespie, P.; Goodnow, R.; Harris, W.; Jones, P.; Taniguchi, M.; Tsujii, S.; von der Saal, W.; Zimmermann, G.; Schneider, G. Development of a virtual screening method for identification of “frequent hitters” in compound libraries. *J. Med. Chem.* **2002**, *45*, 137–142.
- (5) Crisman, T. J.; Parker, C. N.; Jenkins, J. L.; Scheiber, J.; Thoma, M.; Kang, Z. B.; Kim, R.; Bender, A.; Nettles, J. H.; Davies, J. W.; Glick, M. Understanding false positives in reporter gene assays: in silico chemogenomics approaches to prioritize cell-based HTS data. *J. Chem. Inf. Model.* **2007**, *47*, 1319–1327.
- (6) DeWitte, R. S. Avoiding physicochemical artefacts in early ADME-Tox experiments. *Drug Discovery Today* **2006**, *11*, 855–859.
- (7) Feng, B. Y.; Shelat, A.; Doman, T. N.; Guy, R. K.; Shoichet, B. K. High-throughput assays for promiscuous inhibitors. *Nat. Chem. Biol.* **2005**, *1*, 146–148.
- (8) Liu, H. Y.; Wang, Z.; Regni, C.; Zou, X.; Tipton, P. A. Detailed kinetic studies of an aggregating inhibitor; inhibition of phosphomannomutase/phosphoglucomutase by disperse blue 56. *Biochemistry* **2004**, *43*, 8662–8669.
- (9) Reddie, K. G.; Roberts, D. R.; Dore, T. M. Inhibition of kinesin motor proteins by adociasulfate-2. *J. Med. Chem.* **2006**, *49*, 4857–4860.
- (10) Coan, K. E.; Maltby, D. A.; Burlingame, A. L.; Shoichet, B. K. Promiscuous aggregate-based inhibitors promote enzyme unfolding. *J. Med. Chem.* **2009**, *52*, 2067–2075.
- (11) Davies, S. P.; Reddy, H.; Caivano, M.; Cohen, P. Specificity and mechanism of action of some commonly used protein kinase inhibitors. *Biochem. J.* **2000**, *351*, 95–105.
- (12) Lingameneni, R.; Vysotskaya, T. N.; Duch, D. S.; Hemmings, H. C., Jr. Inhibition of voltage-dependent sodium channels by Ro 31-8220, a “specific” protein kinase C inhibitor. *FEBS Lett.* **2000**, *473*, 265–268.
- (13) McGovern, S. L.; Shoichet, B. K. Kinase inhibitors: not just for kinases anymore. *J. Med. Chem.* **2003**, *46*, 1478–1483.
- (14) Coan, K. E.; Shoichet, B. K. Stoichiometry and physical chemistry of promiscuous aggregate-based inhibitors. *J. Am. Chem. Soc.* **2008**, *130*, 9606–9612.
- (15) Seidler, J.; McGovern, S. L.; Doman, T. N.; Shoichet, B. K. Identification and prediction of promiscuous aggregating inhibitors among known drugs. *J. Med. Chem.* **2003**, *46*, 4477–4486.
- (16) Frenkel, Y. V.; Clark, A. D., Jr.; Das, K.; Wang, Y. H.; Lewi, P. J.; Janssen, P. A.; Arnold, E. Concentration and pH dependent aggregation of hydrophobic drug molecules and relevance to oral bioavailability. *J. Med. Chem.* **2005**, *48*, 1974–1983.
- (17) Janssen, P. A.; Lewi, P. J.; Arnold, E.; Daeyaert, F.; de Jonge, M.; Heeres, J.; Koymans, L.; Vinkers, M.; Guillemont, J.; Pasquier, E.; Kukla, M.; Ludovici, D.; Andries, K.; de Bethune, M. P.; Pauwels, R.; Das, K.; Clark, A. D., Jr.; Frenkel, Y. V.; Hughes, S. H.; Medaer, B.; De Knaep, F.; Bohets, H.; De Clerck, F.; Lampo, A.; Williams, P.; Stoffels, P. In search of a novel anti-HIV drug: multidisciplinary coordination in the discovery of 4-[[4-[(1E)-2-cyanoethenyl]-2,6-dimethylphenyl]amino]-2-pyrimidinyl]amino]benzotrile (R278474, rilpivirine). *J. Med. Chem.* **2005**, *48*, 1901–1909.
- (18) Lewi, P.; Arnold, E.; Andries, K.; Bohets, H.; Borghys, H.; Clark, A.; Daeyaert, F.; Das, K.; de Bethune, M. P.; de Jonge, M.; Heeres, J.; Koymans, L.; Leempoels, J.; Peeters, J.; Timmerman, P.; Van den Broeck, W.; Vanhoutte, F.; Van't Klooster, G.; Vinkers, M.; Volovik, Y.; Janssen, P. A. Correlations between factors determining the pharmacokinetics and antiviral activity of HIV-1 non-nucleoside reverse transcriptase inhibitors of the diarylthiazine and diarylpyrimidine classes of compounds. *Drugs R&D* **2004**, *5*, 245–257.
- (19) Coan, K. E.; Shoichet, B. K. Stability and equilibria of promiscuous aggregates in high protein milieus. *Mol. Biosyst.* **2007**, *3*, 208–213.
- (20) Flynn, B. C.; Sladen, R. N. The use of methylene blue for vasodilatory shock in a pediatric lung transplant patient. *J. Cardiothorac. Vasc. Anesth.* **2009**, *23*, 529–530.
- (21) Oz, M.; Lorke, D. E.; Petroianu, G. A. Methylene blue and Alzheimer's disease. *Biochem. Pharmacol.* **2009**, *78*, 927–932.
- (22) Wainwright, M. The use of dyes in modern biomedicine. *Biotech. Histochem.* **2003**, *78*, 147–155.
- (23) Ryan, A. J.; Gray, N. M.; Lowe, P. N.; Chung, C. W. Effect of detergent on “promiscuous” inhibitors. *J. Med. Chem.* **2003**, *46*, 3448–3451.
- (24) Jadhav, A.; Ferreira, R. S.; Klumpp, C.; Mott, B. T.; Austin, C. P.; Ingles, J.; Thomas, C. J.; Maloney, D. J.; Shoichet, B. K.; Simeonov, A. Quantitative analyses of aggregation, autofluorescence, and reactivity artifacts in a screen for inhibitors of a thiol protease. *J. Med. Chem.* **2009**, *53*, 37–51.
- (25) Feng, B. Y.; Shoichet, B. K. A detergent-based assay for the detection of promiscuous inhibitors. *Nat. Protoc.* **2006**, *1*, 550–553.
- (26) Custodio, J. M.; Wu, C. Y.; Benet, L. Z. Predicting drug disposition, absorption/elimination/transporter interplay and the role of food on drug absorption. *Adv. Drug Delivery Rev.* **2008**, *60*, 717–733.
- (27) Dressman, J. B.; Reppas, C. In vitro–in vivo correlations for lipophilic, poorly water-soluble drugs. *Eur. J. Pharm. Sci.* **2000**, *11* (Suppl. 2), S73–S80.
- (28) Jantratic, E.; Janssen, N.; Reppas, C.; Dressman, J. B. Dissolution media simulating conditions in the proximal human gastrointestinal tract: an update. *Pharm. Res.* **2008**, *25*, 1663–1676.
- (29) Sutton, S. C. Role of physiological intestinal water in oral absorption. *AAPS J.* **2009**, *11*, 277–285.
- (30) Marciani, L.; Foley, S.; Hoad, C.; Campbell, E.; Totman, J.; Armstrong, A.; Manby, P.; Gowland, P. A.; Spiller, R. Effects of Ondansetron on Small Bowel Water Content: A Magnetic Resonance Imaging Study. Presented at the 15th United European Gastroenterology Week, Paris, October 27–31, **2007**.
- (31) Marciani, L.; Foley, S.; Hoad, C.; Campbell, E.; Totman, J.; Cox, E.; Gowland, P.; Spiller, R. C. Magnetic Resonance Imaging of Abnormalities in Diarrhoea-Predominant Irritable Bowel Syndrome Fasting and after a Bran-Containing Meal. Presented at the 15th United European Gastroenterology Week, Paris, October 27–31, **2007**.
- (32) Schiller, C.; Frohlich, C. P.; Giessmann, T.; Siegmund, W.; Monnikes, H.; Hosten, N.; Weitschies, W. Intestinal fluid volumes and transit of dosage forms as assessed by magnetic resonance imaging. *Aliment. Pharmacol. Ther.* **2005**, *22*, 971–979.
- (33) Galia, E.; Nicolaidis, E.; Horter, D.; Lobenberg, R.; Reppas, C.; Dressman, J. B. Evaluation of various dissolution media for predicting in vivo performance of class I and II drugs. *Pharm. Res.* **1998**, *15*, 698–705.
- (34) Kostewicz, E. S.; Brauns, U.; Becker, R.; Dressman, J. B. Forecasting the oral absorption behavior of poorly soluble weak bases using solubility and dissolution studies in biorelevant media. *Pharm. Res.* **2002**, *19*, 345–349.
- (35) Nicolaidis, E.; Galia, E.; Efthymiopoulos, C.; Dressman, J. B.; Reppas, C. Forecasting the in vivo performance of four low solubility drugs from their in vitro dissolution data. *Pharm. Res.* **1999**, *16*, 1876–1882.
- (36) Lipinski, C. A.; Lombardo, F.; Dominy, B. W.; Feeney, P. J. Experimental and computational approaches to estimate solubility and permeability in drug discovery and development settings. *Adv. Drug Delivery Rev.* **2001**, *46*, 3–26.
- (37) Mott, B. T.; Ferreira, R. S.; Simeonov, A.; Jadhav, A.; Ang, K. K.; Leister, W.; Shen, M.; Silveira, J. T.; Doyle, P. S.; Arkin, M. R.; McKerrow, J. H.; Ingles, J.; Austin, C. P.; Thomas, C. J.; Shoichet, B. K.; Maloney, D. J. Identification and optimization of inhibitors of trypanosomal cysteine proteases: cruzain, rhodesain, and TbCatB. *J. Med. Chem.* **2009**, *53*, 52–60.
- (38) Wille, H.; Govaerts, C.; Borovinskiy, A.; Latawiec, D.; Downing, K. H.; Cohen, F. E.; Prusiner, S. B. Electron crystallography of the scrapie prion protein complexed with heavy metals. *Arch. Biochem. Biophys.* **2007**, *467*, 239–248.